JOURNAL OF APPLIED PHYSICS VOLUME 93, NUMBER 10 15 MAY 2003

Theoretical and experimental studies of cyclotron resonance in *p*-type InAs and InMnAs at ultrahigh magnetic fields

G. D. Sanders, Y. Sun, and C. J. Stanton
Department of Physics, University of Florida, Gainesville, Florida 32611-8440

G. A. Khodaparast and J. Kono[a)]
Department of Electrical and Computer Engineering, Rice University, Houston, Texas 77005

Y. H. Matsuda[b)] and N. Miura
Institute for Solid State Physics, University of Tokyo, Kashiwa, Chiba 277-8581, Japan

T. Slupinski, A. Oiwa, and H. Munekata
Imaging Science and Engineering Laboratory, Tokyo Institute of Technology, Yokohama, Kanagawa 226-8503, Japan

(Presented on 12 November 2002)

We report theoretical and experimental ultrahigh magnetic field cyclotron resonance (CR) studies of paramagnetic *p*-type InAs and InMnAs. Experimental results are compared with an 8 band Pidgeon–Brown model which includes (i) the wave vector dependence of the electronic states along the magnetic field, and (ii) $s-d$ and $p-d$ exchange interactions with Mn ions. CR spectra are computed using Fermi's golden rule. Results show two strong peaks associated with heavy and light hole transitions. Line shapes of the transitions provide information on the carrier densities. © *2003 American Institute of Physics.* [DOI: 10.1063/1.1556157]

Magnetic semiconductors of $\mathrm{In}_{1-x}\mathrm{Mn}_x\mathrm{As}$ have recently attracted much attention both experimentally and theoretically. Narrow gap materials involve conduction and valence band mixing and Mn doping gives rise to enhanced g factors for both electrons and holes. The electronic and optical properties of $\mathrm{In}_{1-x}\mathrm{Mn}_x\mathrm{As}$ are important for designing ferromagnetic heterostructures and spintronic devices.

We have performed cyclotron resonance experiments on *p*-doped InAs and InMnAs at ultrahigh magnetic fields up to 150 T. In addition, we have developed a theory for electronic and magneto-optical properties of these dilute magnetic semiconductors in ultrahigh magnetic fields, B, oriented along [001]. Our theory builds on the 8 band effective mass Pidgeon–Brown model[1] which we have generalized to include (i) energies and electronic states as a function of the wave vector parallel to B, and (ii) $s-d$ and $p-d$ exchange interactions with Mn d electrons. The exchange coupling is parametrized by exchange integrals α and β defined in Ref. 2. In the paramagnetic phase the magnetization is given by a Brillouin function.[3] We do not take into account changes in band gap or optical matrix element with Mn doping, since this is not well known for InMnAs systems. Magneto-optical properties and cyclotron resonance are obtained using Fermi's golden rule to compute the dielectric function.[4] Band filling effects are explicitly considered and the Dirac delta functions appearing in the golden rule transition rates are replaced by Lorentzian line shapes with the full width at half maximum (FWHM) being an input parameter.

Results for *n*-type systems have been discussed previously.[5–7] In this article, we concentrate on *p*-type systems. In Fig. 1(a) experimental and theoretical cyclotron resonance absorption curves (solid lines) are plotted as a function of the applied magnetic field in *p*-doped InAs. The radiation is *h*-active circularly polarized with photon energy

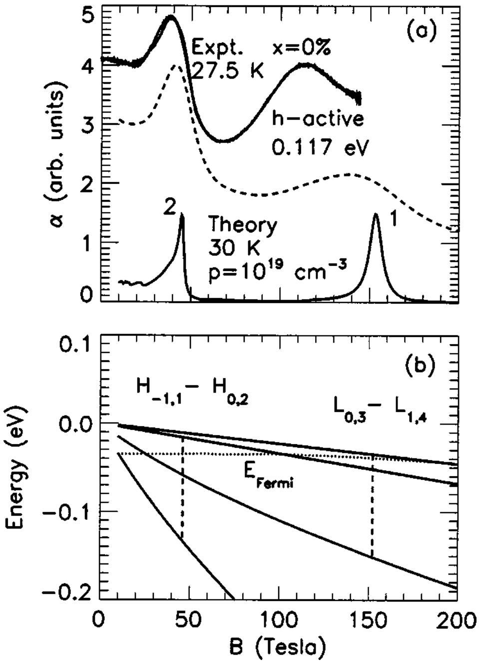

FIG. 1. (a) Cyclotron absorption as a function of B in *p*-type InAs for *h*-active circularly polarized light with $\hbar\omega=0.117$ eV. The solid theory curve is broadened with a minimal 4 meV linewidth while the dashed theory curve is broadened with a 40 meV linewidth. (b) The $k=0$ energies of Landau subbands responsible for peaks 1 and 2.

[a)] Author to whom correspondence should be addressed; electronic mail: kono@rice.edu

[b)] Present address: Department of Physics, Okayama University, Okayama, Japan.

0021-8979/2003/93(10)/6897/3/$20.00

© 2003 American Institute of Physics

Downloaded 31 Dec 2010 to 168.7.222.153. Redistribution subject to AIP license or copyright; see http://jap.aip.org/about/rights_and_permissions

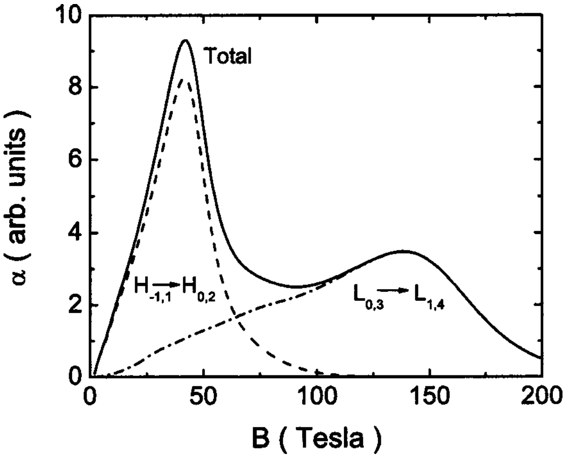

FIG. 2. Theoretically computed cyclotron absorption only from the $H_{-1,1}-H_{0,2}$ and $L_{0,3}-L_{1,4}$ transitions (with 40 meV broadening). The experimental situation is the same as in Fig. 1. Comparing the results to Fig. 1, we see that all the cyclotron resonance above 30 T is accounted for by these transitions. Below 30 T, higher Landau level transitions contribute to the background absorption.

$\hbar\omega=0.117$ eV. In the theoretical cyclotron resonance, the FWHM linewidth is taken to be $\gamma=4$ meV which is narrower than in the experimental situation. The dashed curve shows the theoretical cyclotron resonance broadened with $\gamma=40$ meV which more closely approximates the experiment. The carrier density in the theoretical calculation is $p=10^{19}\,\mathrm{cm}^{-3}$ so that for $T=30\,\mathrm{K}$ and $B>30\,\mathrm{T}$, the Fermi energy is such that even at high magnetic fields (150 T) the first two Landau subbands are still occupied. For calculations with a density of $p=5\times10^{18}\,\mathrm{cm}^{-3}$ only the lowest transition peak occurs indicating that the experimental carrier density must be greater than this.

Holes optically excited from these two subbands give rise to the two strong cyclotron absorption peaks labeled 1 and 2. The zone center Landau subband energies involved in these two cyclotron resonance transitions are shown in Fig. 1(b). The cyclotron absorption peak, 2, near 40 T, is due to a transition between the spin down ground state heavy hole Landau subband, $H_{-1,1}$, with energy $E_{-1,1}(k_z)$ and the Landau subband, $H_{0,2}$, with energy $E_{0,2}(k_z)$. Landau energies are labeled $E_{n,v}(k_z)$ where $(n=-1,...,\infty)$ labels the Landau levels and v labels energies with the same n in ascending order.[2] Near the zone center $H_{0,2}$ is primarily spin down heavy hole in character which accounts for our use of the "*H*" designation for this subband. The cyclotron absorption peak, 1, around 140 T, is a spin down light hole transition between the $L_{0,3}$ and $L_{1,4}$ levels. While the theoretical peak does not fit the experimental peak exactly, by varying the Luttinger parameter γ_1, the peak position can be changed and brought into better agreement with the experiment. This shows that ultrahigh magnetic field cyclotron resonance experiments can be used to accurately determine the band parameters and effective masses. The peaks 1 and 2 are seen to be asymmetric about their respective resonance fields. For $B<30\,\mathrm{T}$, higher Landau subbands become occupied and excitation of holes from these subbands is responsible for the downward sloping plateau seen in the experimental cyclotron resonance absorption.

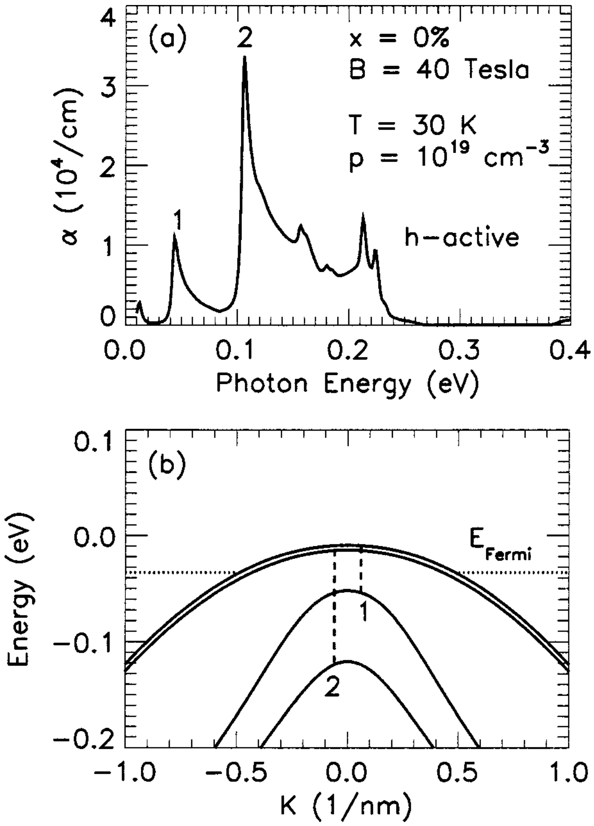

FIG. 3. (a) The *h*-active circularly polarized absorption for *p*-InAs in an external field $B=40\,\mathrm{T}$ at $T=30\,\mathrm{K}$. The hole concentration $p=10^{19}\,\mathrm{cm}^{-3}$. Two main absorption peaks 1 and 2 are indicated. Other peaks correspond to transitions between higher occupied Landau levels. (b) The valence subbands responsible for the absorption peaks 1 and 2.

In Fig. 2, we plot contributions to the total cyclotron resonance in Fig. 1 due to the two dominant transitions $H_{-1,1}-H_{0,2}$ and $L_{0,3}-L_{1,4}$. Comparing Fig. 1 and Fig. 2, we see that for $B>30\,\mathrm{T}$ the cyclotron resonance (CR) signal can be accounted for by these two transitions. At low magnetic fields, higher Landau levels are occupied (cf. Fig. 1) giving rise to the low field background.

In Fig. 3 we set the magnetic field to $B=40\,\mathrm{T}$ which is close to the resonance field for the $H_{-1,1}-H_{0,2}$ cyclotron resonance peak (peak 2) in Fig. 1 and scan the laser absorption frequency ω. Figure 3(a) shows the *h*-circularly polarized absorption spectrum in *p*-type InAs for $p=10^{19}\,\mathrm{cm}^{-3}$ and $T=30\,\mathrm{K}$. We find that the six lowest Landau levels are occupied giving rise to the six peaks seen in the absorption spectrum. The most pronounced absorption peaks are the two lowest ones labeled 1 and 2 in Fig. 3(a). As expected, peak 2 in the absorption spectrum occurs at a photon energy of $\hbar\omega=0.117$ eV. In Fig. 3(b), the valence subband levels responsible for these two main peaks are shown as functions of the wave vector k_z in the direction of the magnetic field. The asymmetry of the line shapes of peaks 1 and 2 in Fig. 3(a) is primarily due to the joint density of states of the subbands involved in the two transitions. As the laser frequency ω is increased, the optical transition occurs further away from the zone center along the k_z direction and owing to the different

Downloaded 31 Dec 2010 to 168.7.222.153. Redistribution subject to AIP license or copyright; see http://jap.aip.org/about/rights_and_permissions

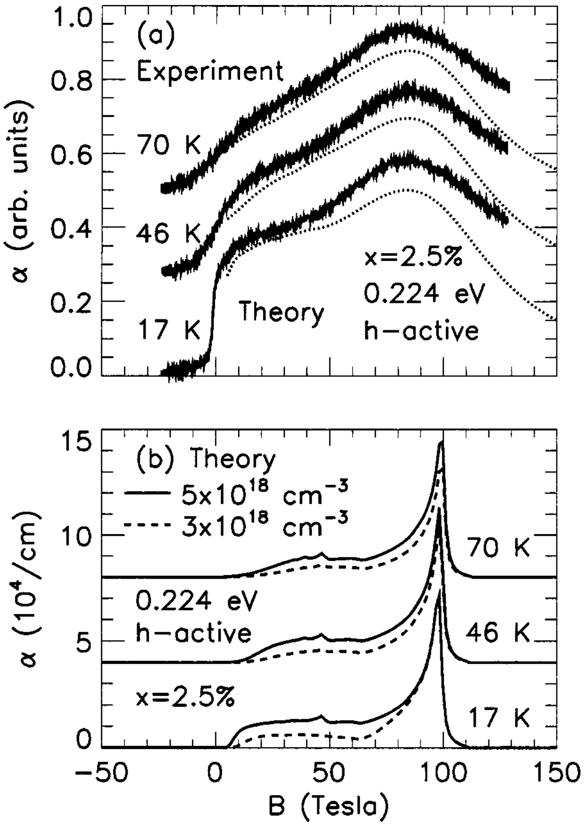

FIG. 4. (a) Experimental (solid lines) and theoretical (dotted lines) *h*-active CR absorption for $\hbar\omega$=0.224 eV vs magnetic field in p-In$_{0.975}$Mn$_{0.025}$As at 17, 46 and 70 K. The theoretical curves have FWHM linewidths of 120 meV and $p=5\times10^{18}\,\mathrm{cm}^{-3}$. (b) Theoretical absorption spectra as in (a) with FWHM linewidths of 4 meV and $p=3\times10^{18}\,\mathrm{cm}^{-3}$ and $p=5\times10^{18}\,\mathrm{cm}^{-3}$.

curvatures of the subbands, the joint density of states changes.

CR absorption measurements were also performed on an In$_{1-x}$Mn$_x$As sample with $x=2.5\%$. The CR measurements were made at temperatures of 17, 46, and 70 K in *h*-active circularly polarized light with $\hbar\omega$=0.224 eV. In Fig. 4(a), the experimental CR is shown as a function of the magnetic field for the three temperatures and the corresponding theoretical CR absorption spectra are shown as dotted lines. In the theory curves in Fig. 4(a), the FWHM linewidths are taken to be 120 meV and the hole concentration is taken to be $p=5\times10^{18}\,\mathrm{cm}^{-3}$. In Fig. 4(b), we reduce the FWHM linewidths to 4 meV and plot the theoretical CR for hole concentrations of $p=3\times10^{18}\,\mathrm{cm}^{-3}$ and $p=5\times10^{18}\,\mathrm{cm}^{-3}$. A heavy hole CR transition is seen at a resonance field around 80 T. This corresponds to transition 2 seen in Fig. 1 near 40 T. This transition occurs at a higher magnetic field since the energy of the probe laser has changed from 0.117 to 0.224 eV. The resonance field is insensitive to temperature and the line shape is strongly asymmetric with a broad tail at low fields. Note, however, that the width of the low field tail depends on the free hole concentration as seen in Fig. 4(b). Again, the width of the low field tail results from higher order Landau levels being populated. The low field tail is thus a sensitive measurement of the carrier density. In addition, the sharpness of the low field cutoff is seen to depend on temperature and can be attributed to the sharpness of the Fermi distribution at low temperatures. The results show that the cyclotron resonance for the InMnAs case is made up of one strong heavy hole transition together with background absorption due to higher populated Landau levels at low values of the magnetic field.

In summary, we have performed ultrahigh magnetic field cyclotron resonance experiments on *p*-type InAs and InMnAs. Theoretical calculations based on a Pidgeon–Brown model with an $sp-d$ Mn exchange interaction predict two strong transitions in the absorption spectra. These are associated with the heavy hole $H_{-1,1}-H_{0,2}$ and light hole $L_{0,3}-L_{1,4}$ transitions. At low magnetic fields, there are additional transitions associated with the population of higher lying Landau levels. The density dependence of the cyclotron resonance line shape can help one to determine the carrier densities.

This work was supported by DARPA through Grant No. MDA 972-00-1-0034 and the NEDO International Joint Research Program.

[1] C. K. Pidgeon and R. N. Brown, Phys. Rev. **146**, 575 (1966).
[2] J. Kossut, Semicond. Semimetals **25**, 183 (1988).
[3] J. K. Furdyna, J. Appl. Phys. **64**, R29 (1988).
[4] F. Bassani and G. P. Parravicini, *Electronic States and Optical Transitions in Solids* (Pergamon, New York, 1975).
[5] G. D. Sanders, Y. Sun, C. J. Stanton, G. A. Khodaparast, J. Kono, Y. H. Matsuda, N. Miura, T. Slupinski, A. Oiwa, and H. Munekata, J. Supercond. (accepted).
[6] G. A. Khodaparast, M. A. Zudov, J. Kono, Y. H. Matsuda, T. Ikaida, S. Ikeda, N. Miura, T. Slupinski, A. Oiwa, and H. Munekata *et al.*, J. Supercond. (accepted).
[7] M. A. Zudov, J. Kono, Y. H. Matsuda, T. Ikaida, N. Miura, H. Munekata, G. D. Sanders, Y. Sun, and C. J. Stanton, Phys. Rev. B **66**, 161307(R) (2002).

Downloaded 31 Dec 2010 to 168.7.222.153. Redistribution subject to AIP license or copyright; see http://jap.aip.org/about/rights_and_permissions